

Supplementary Information

for

A Cu^{II} complex of emodin improves upon the anticancer activity of the molecule as demonstrated by its performance on HeLa and Hep G2 cells

Bitapi Mandal, Soumen Singha, Sanjay Kumar Dey, Swagata Mazumdar,

Sanjay Kumar, Parimal Karmakar, Saurabh Das^{*}

Experimental:

Determination of the stoichiometry of the Cu^{II} complex of emodin (LH₃)

Mole-ratio method:

The concentration of Cu(II) was constant while emodin was varied. The change in absorbance at 536 nm was plotted against the changing ratio of emodin (LH₃) to Cu(II) at a constant metal ion concentration [Fig. S1(a)]. Straight lines were obtained whose intersection provides the stoichiometry of complex formation in solution.

Job's method of continuous variation:

Stoichiometry was also determined by continuously varying the concentration of both the ligand (emodin) and Cu(II) [Fig. S1(b)].

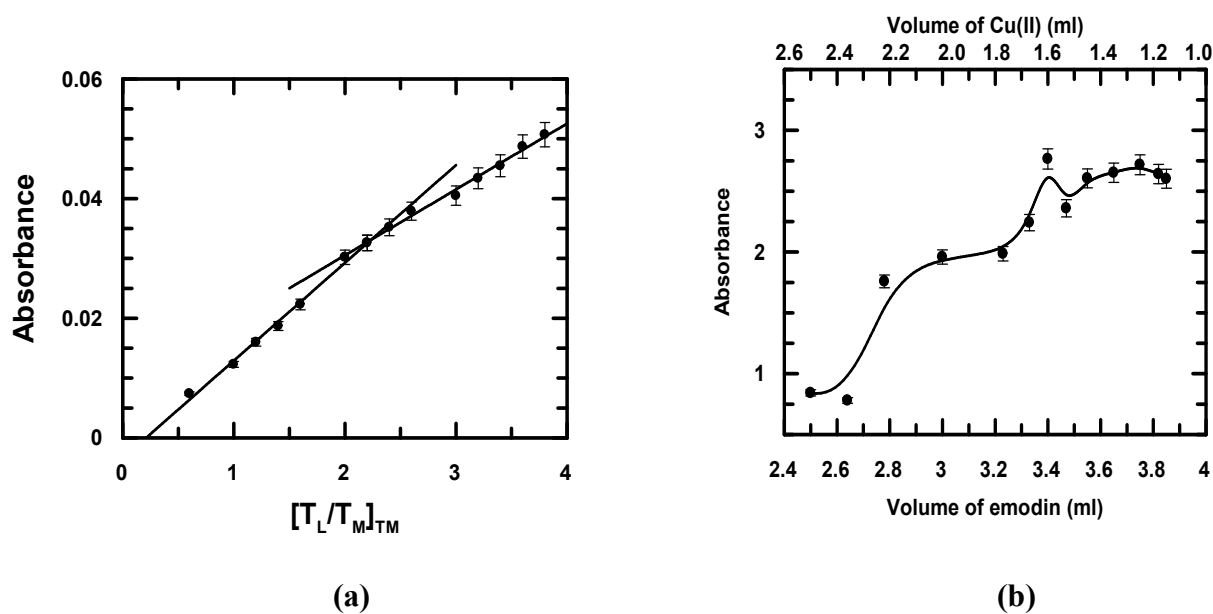


Fig. S1: (a) Mole-ratio plot showing interaction of Cu(II) with emodin in solution at neutral pH; (b) Job's plot of continuous variation showing interaction of Cu(II) with emodin at neutral pH. $[\text{NaNO}_3] = 100 \text{ mM}$, Temperature = 298 K.

Both methods suggest the formation of a 1:2 metal-ligand complex at neutral pH.

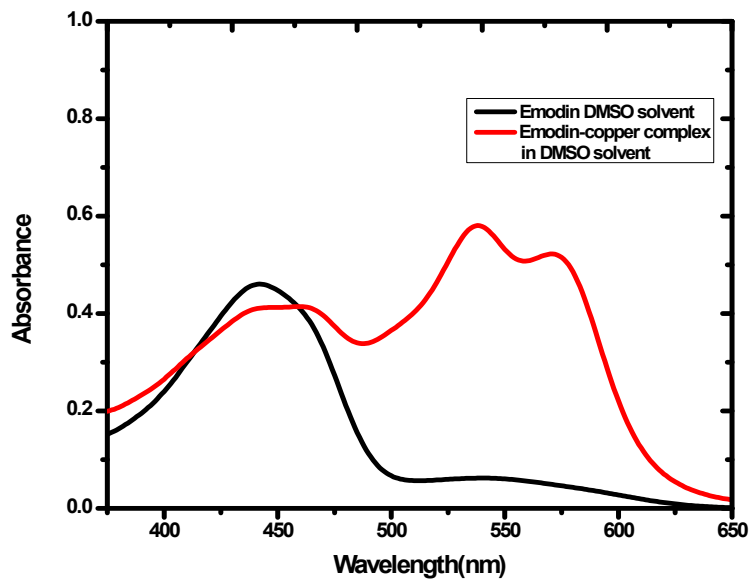


Fig. S2: UV-Vis spectra of emodin and its Cu(II) complex in DMSO

Analysis of IR spectra:

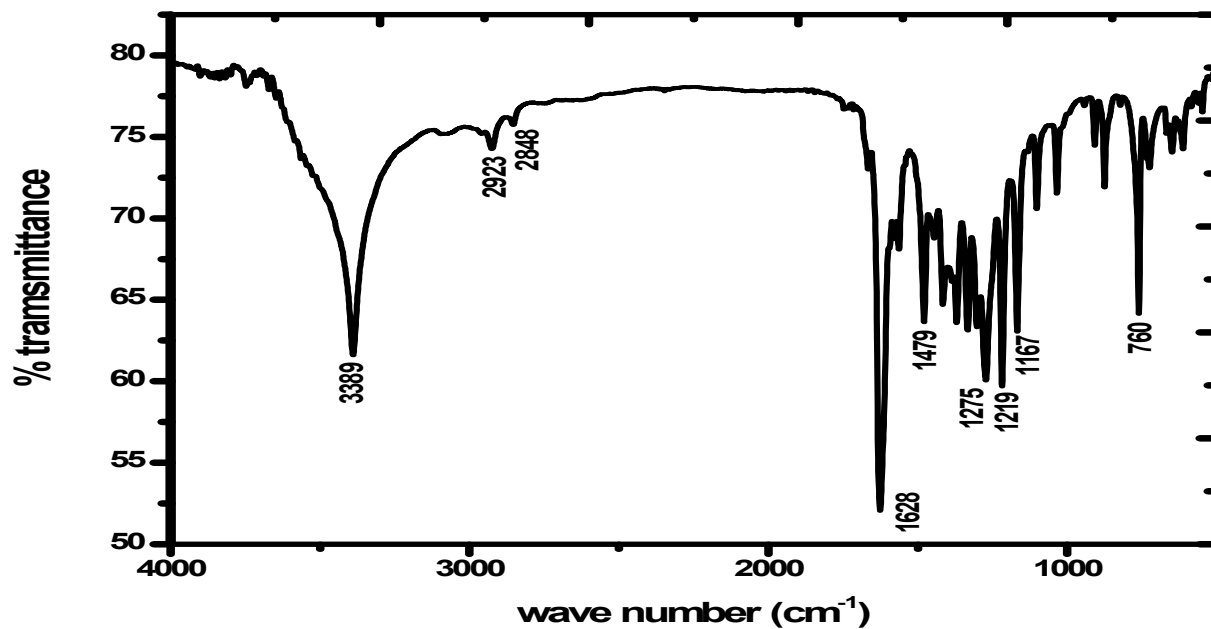


Fig. S3: IR spectra of emodin

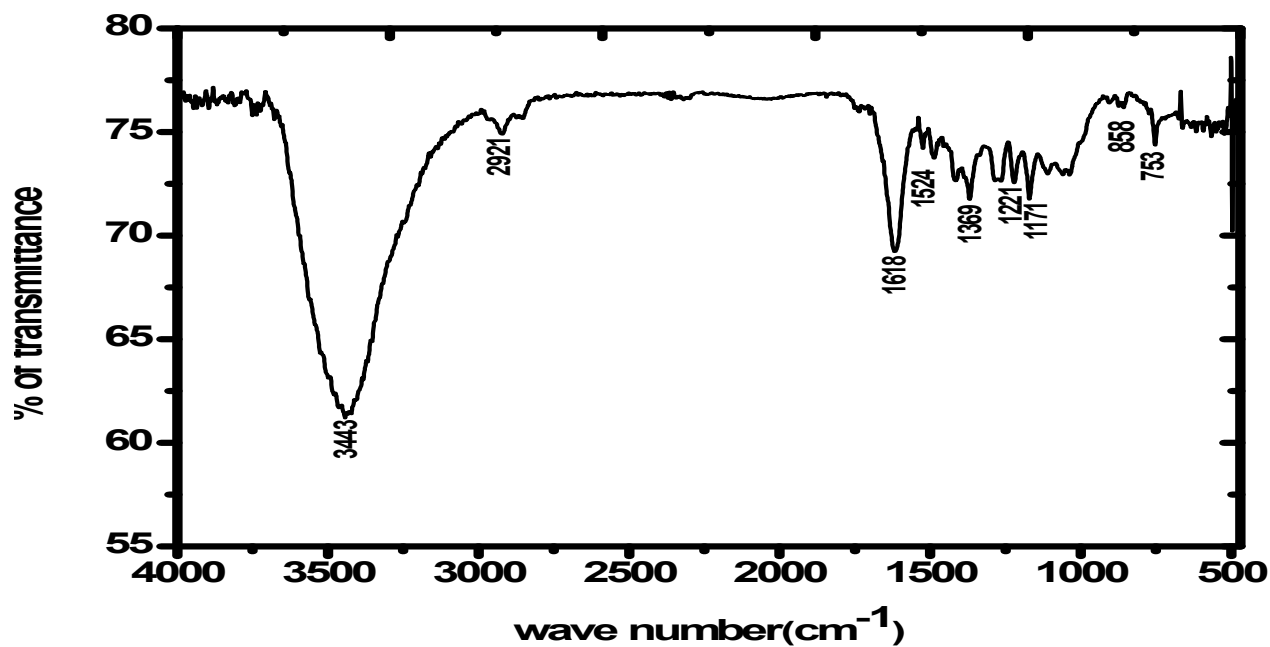


Fig. S4: IR spectrum of $[\text{Cu}^{\text{II}}(\text{emod})_2]^{2-}$

Analysis of the IR spectrum of emodin (Fig. S3) and the Cu(II) complex (Fig. S4) reveals that the sharp peak at 3389 cm^{-1} for emodin broadens in case of the complex being shifted to 3443 cm^{-1} . The peak for emodin is attributed to -OH stretching due to strong intra-molecular hydrogen bonding for the -OH group at C_1 and C_8 with the adjacent carbonyl group at C_9 . In Cu(II)-emodin, broadening of peak at 3443 cm^{-1} occurs due to the absence of intramolecular H-bonding between adjacent -OH and C=O groups following introduction of the metal ion. Carbonyl stretching was found at 1628 cm^{-1} for emodin and at 1618 cm^{-1} for the complex suggestive of the fact that while one carbonyl per ligand is bound to metal ion in the complex, the other carbonyl retains its character. There was significant differences in the region from 1480 cm^{-1} to 700 cm^{-1} for emodin and its Cu(II) complex suggesting complex formation.

Mass Spectrum:

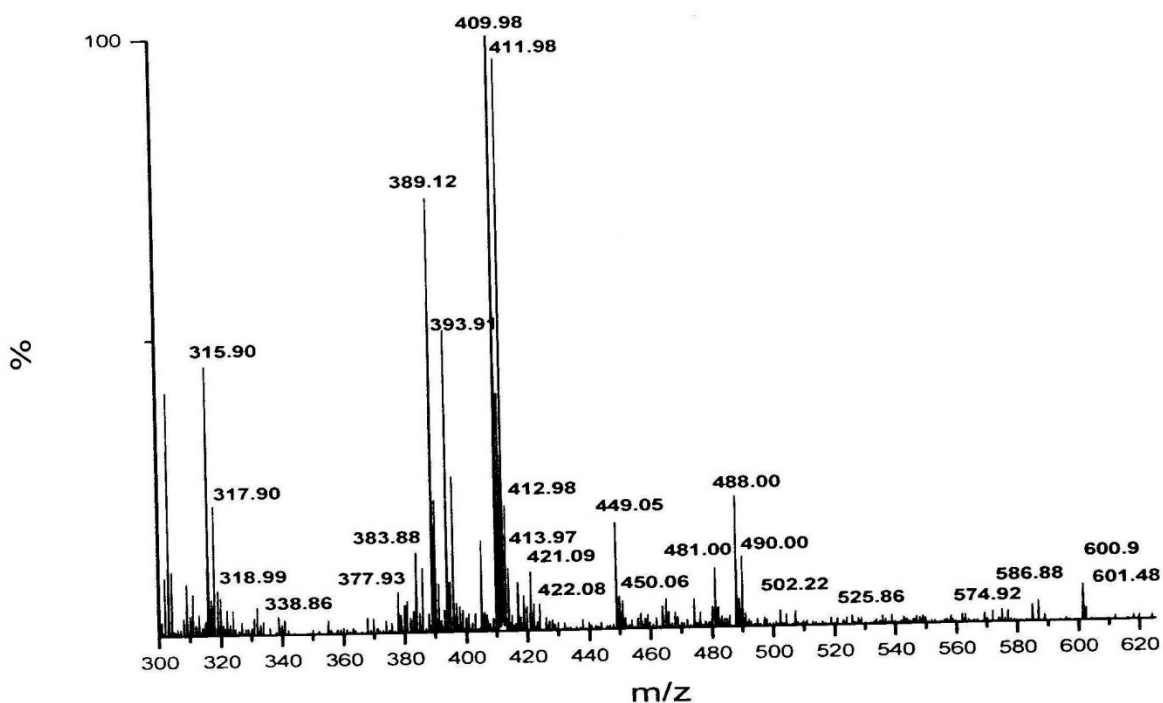


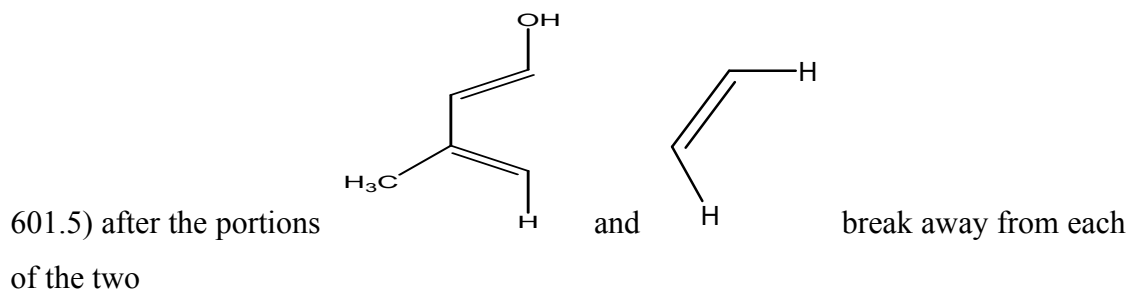
Fig. S5: Mass spectrum of $[\text{Cu}^{\text{II}}(\text{emod})_2]^{2-}$

Analysis of Mass spectrum:

The molecular ion peak was detected at $m/z = 600.9$ and 601.48 ($m/z_{\text{theo}} = 599.48$ & 601.48 considering ^{63}Cu and ^{65}Cu respectively). The peaks at $m/z = 586.88$ and 574.92 corresponds to

the loss of either one or two methyl groups from the two emodin units in the complex in succession [m/z_{theo} being 585.48 (^{63}Cu), 587.48 (^{65}Cu) and 571.48 (^{63}Cu), 573.48 (^{65}Cu)]. Peaks in the region of $m/z = 525.86$ corresponds to a fragment formed by further loss of one -OH group and one O^- unit from each emodin in the complex.

The peak at $m/z = 393.91$ corresponds to the fragment formed from the molecular ion ($m/z =$



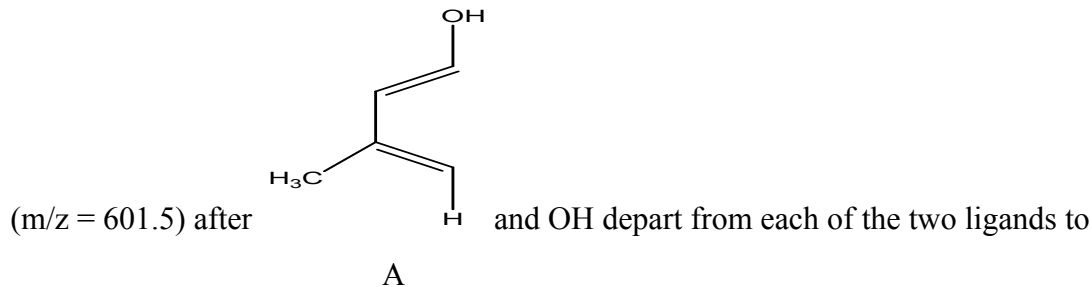
ligands to result in a fragment 393.91 (theoretical $m/z = 393.5$).

Theoretically, the fragment formation can be shown as

$$601.5 - 2 (\text{A}) - 2 (\text{B}) + 8 = 393.5$$

The peak at $m/z = 389.12$ is the same fragment as that of 393.91 but with four H atoms less i.e. theoretically $601.5 - 2 (\text{A}) - 2 (\text{B}) + 8 - 4 = 389.5$.

The peak at $m/z = 409.98$ corresponds to the fragment formed from the molecular ion



result in a fragments having $m/z = 409.98$ and 411.98 respectively (theoretical $m/z = 409.5$ and 411.5 respectively) being the isotopic distributions due to ^{63}Cu and ^{65}Cu . Cu^{II} bound to one emodin from which one O^- unit has departed were detected at $m/z = 316.90$, 317.90 and 318.99 (m/z_{theo} being 316.24 & 318.24 for ^{63}Cu and ^{65}Cu respectively).

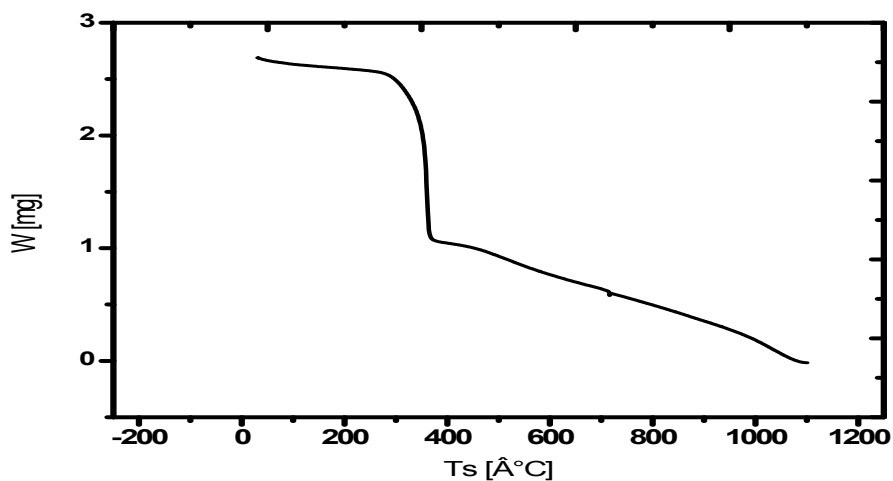
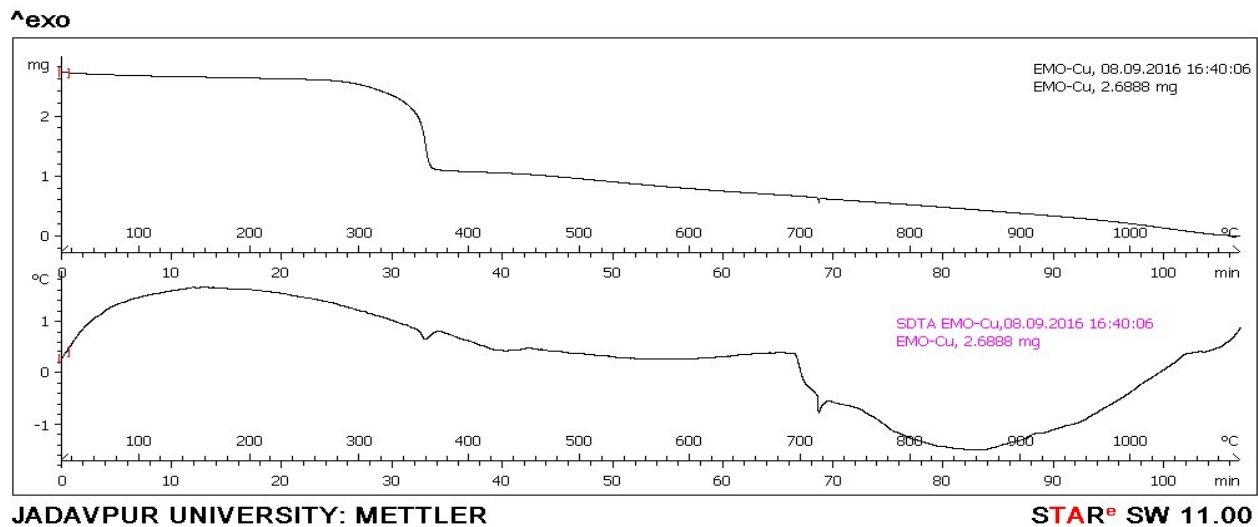


Fig. S6: A routine thermo-gravimetric analysis of Cu^{II}(emod)₂

Thermo-gravimetric analysis:

TGA does not show any loss of material till 200°C indicating no water of crystallization or presence of coordinated water in the complex which is in accordance with the structure obtained from PXRD data.

EPR spectrum of the complex:

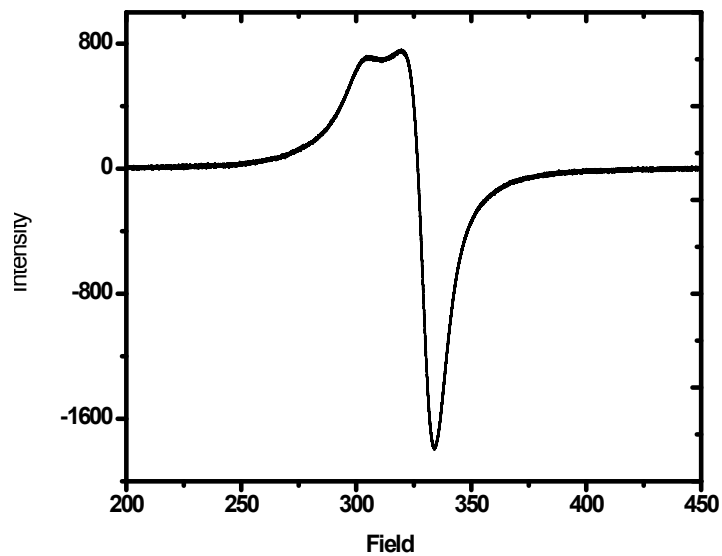


Fig. S7: EPR spectrum of $\text{Cu}^{\text{II}}(\text{emod})_2$

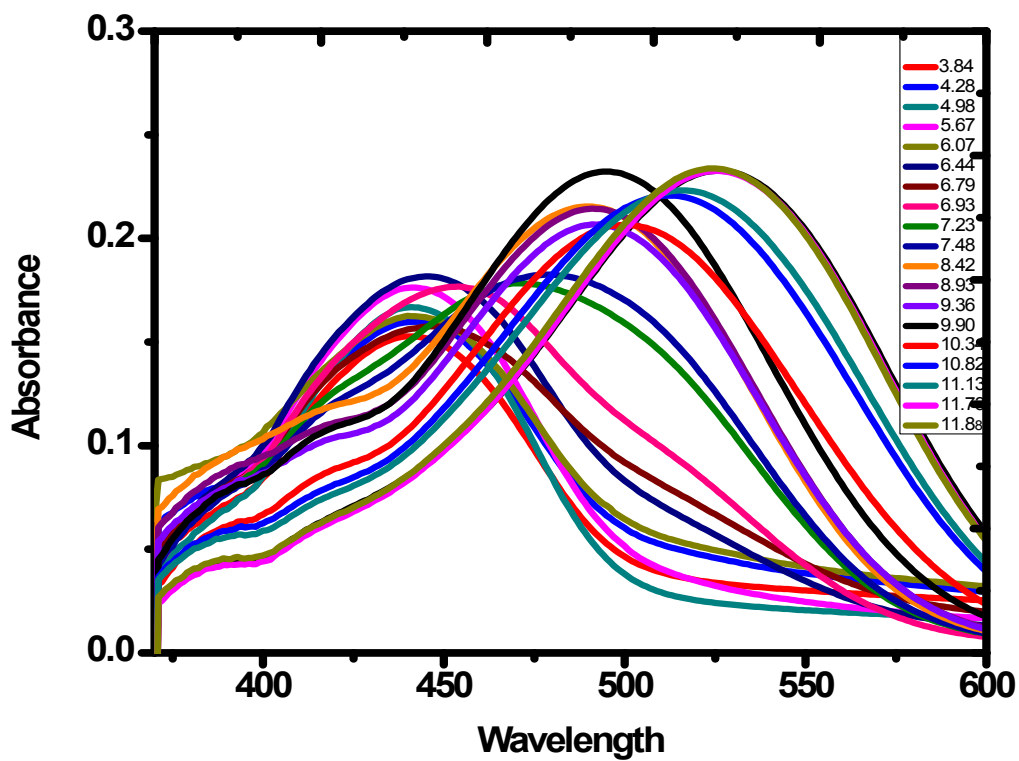
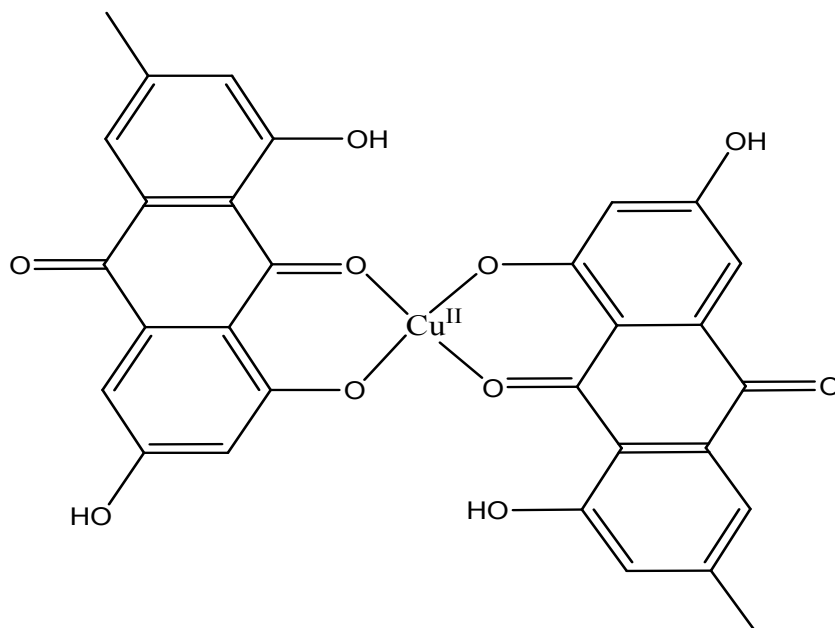


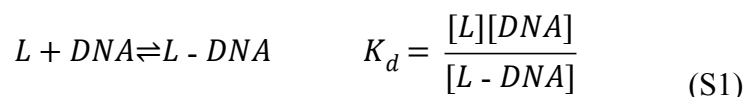
Fig. S8: Absorption spectra of emodin in aqueous solution at different pH; pH of each solution is mentioned in the inset of the figure. $[\text{Emodin}] = 10 \mu\text{M}$, $[\text{NaNO}_3] = 0.01\text{M}$, Temperature = 300 K.

The initial structural model for $[\text{Cu}^{\text{II}}(\text{emod})_2]$ that was used to arrive at the structure of the complex from PXRD data is provided below:



Interaction of the compounds with DNA

Binding of the compounds with calf thymus DNA was studied considering the following equilibrium



Equation S1 considered in the reverse direction yields a double reciprocal equation (S2).

$$\frac{1}{\Delta A} = \frac{1}{\Delta A_{\max}} + \frac{K_d}{\Delta A_{\max}(C_D - C_L)} \quad (\text{S2})$$

Decrease in absorbance (ΔA) upon titration of the compounds with calf thymus DNA was used to create binding isotherms at different ionic strength of the medium when temperature remained constant and at different temperatures when ionic strength of the medium remained constant [1-4]. ΔA_{\max} is the maximum change in absorbance following interaction of the compounds with

calf thymus DNA. C_D denotes the concentration of calf thymus DNA and C_L the concentration of the compounds. K_d and ΔA_{max} were evaluated utilizing Eq. S2.

Change in absorbance following interaction with calf thymus DNA was followed at the λ_{max} of the compounds. A typical double reciprocal plot from where K_d and ΔA_{max} were evaluated allows us to plot of $\Delta A/\Delta A_{max}$ against concentration of DNA. This was fitted using the non-linear curve fit analysis (Eq. S3 & S4) and K_d was evaluated once again.

$$K_d = \frac{\left[C_L - \left(\frac{\Delta A}{\Delta A_{max}} \right) C_L \right] \left[C_D - \left(\frac{\Delta A}{\Delta A_{max}} \right) C_L \right]}{\left(\frac{\Delta A}{\Delta A_{max}} \right) C_L} \quad (S3)$$

$$C_L \left(\frac{\Delta A}{\Delta A_{max}} \right)^2 - (C_L + C_D + K_d) \left(\frac{\Delta A}{\Delta A_{max}} \right) + C_D = 0 \quad (S4)$$

The plot of $\Delta A/\Delta A_{max}$ against $[DNA]/[compounds]$ provides “ n_b ” the site size of interaction. The overall binding constant (K^*) was obtained by multiplying K_{app} that was obtained from Eq. S2 and Eqs. S3 & S4) with “ n_b ”. A modified form of the original Scatchard equation (Eq. S5) [5] was also used to analyze the titration results. Overall binding constant (K^*) and binding stoichiometry “ n ” ($= n_b^{-1}$) were obtained directly from the equation [1, 6].

$$r/C_f = K^* (n - r) \quad (S5)$$

$r = C_b/C_D$ where, “ C_b ” is the concentration of bound compound, “ C_D ” the concentration of calf thymus DNA and “ C_f ” the concentration of free compound in solution. K^* is the intrinsic or overall binding constant of a compound binding to a substrate. “ n ” is the binding stoichiometry

in terms of the number of compound bound per nucleotide while “ n_b ” reciprocal of “ n ” denotes binding site size in terms of the number of nucleotide bound to a compound.

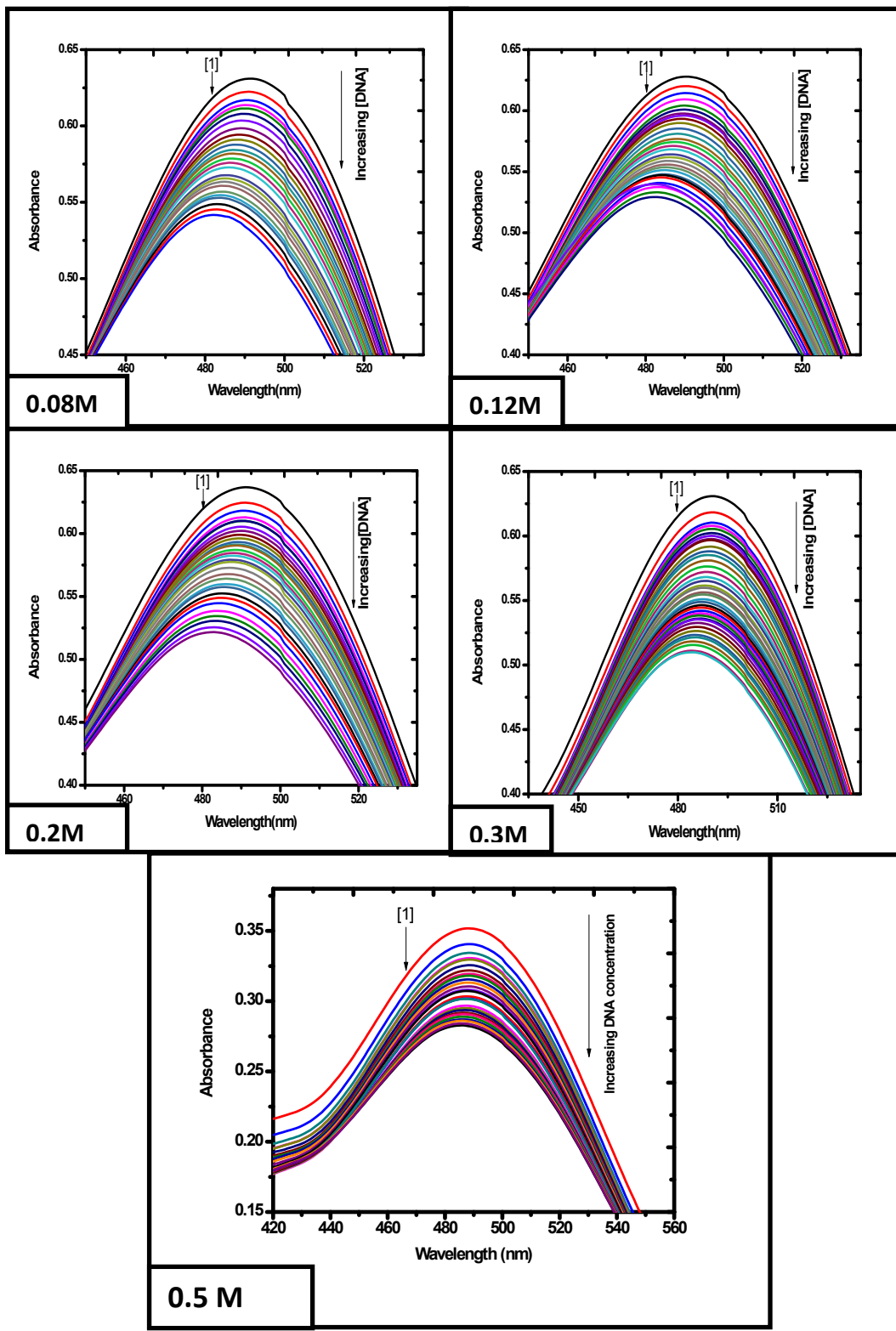


Fig. S9: Absorption spectra of $[\text{Cu}^{\text{II}}(\text{emod})_2]^{2-}$ in the absence (1) and presence of calf thymus DNA. Spectra were recorded at different ionic strengths of the medium showing a gradual decrease in absorbance upon adding DNA to an aqueous solution of the compound. $[\{\text{Cu}^{\text{II}}(\text{emod})_2\}^{2-}] = 50\mu\text{M}$; $[\text{NaCl}] = 120\text{ mM}$; $[\text{Tris buffer}] = 20\text{mM}$, $T = 298\text{ K}$.

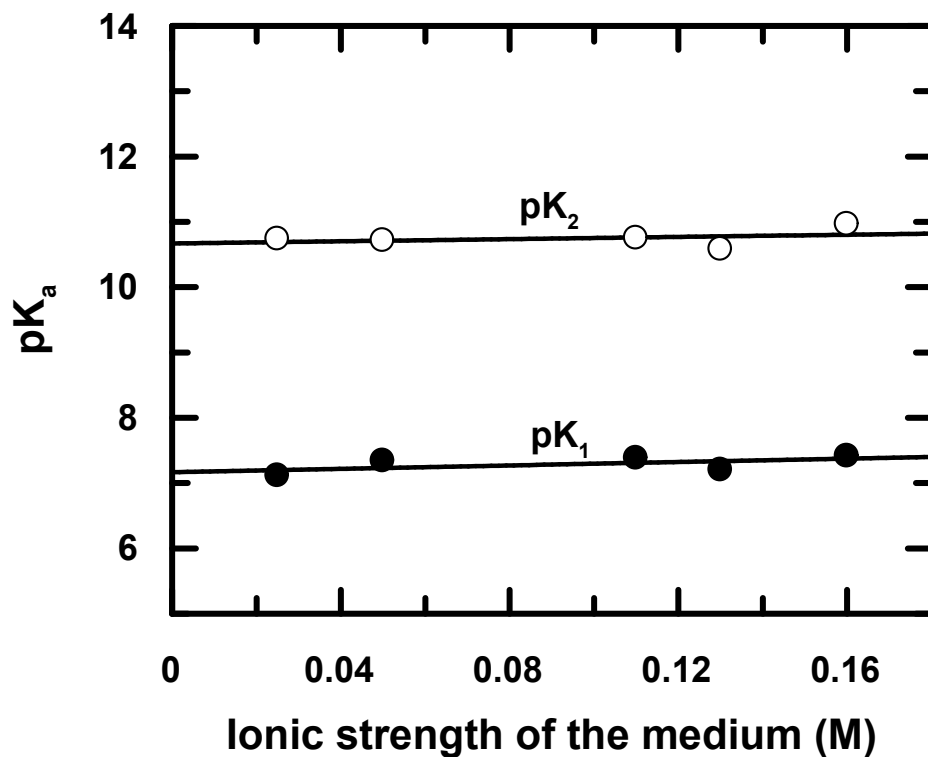


Fig. S10: Linear dependence of pK values of Emodin with a variation in the ionic strength of the medium at 298 K; $[\text{Emodin}] = 10\mu\text{M}$.

References:

- 1) P. S. Guin, S. Das, P. C. Mandal, *J. Inorg. Biochem.* 103 (2009) 1702.
- 2) S. Mukherjee, P. Das, S. Das, *J. Phy.Org. Chem.* 25 (2012) 385.
- 3) S. Roy, R. Banerjee, M. Sarkar, *J. Inorg. Biochem.* 100 (2006) 1320.
- 4) S. Chakraborti, B. Bhattacharyya, D. Dasgupta, *J. Phys. Chem. B* 106 (2002) 6947.
- 5) G. Scatchard, *Ann. N. Y. Acad. Sci.* 51 (1949) 660.
- 6) P. Das, P. S. Guin, P. C. Mandal, M. Paul, S. Paul, S. Das, *J. Phy.Org. Chem.* 24 (2011) 774.
- 7) S. Das, A. Saha, P. C. Mandal, *Talanta* 43 (1996) 95.
- 8) H. Beraldo, A. G. Suillerot, L. Tosi, *Inorg. Chem.* 22 (1983) 4117.
- 9) R.G. Parr, W. Yang, *Density Functional Theory of Atoms and Molecules*, Oxford University Press, Oxford, 1989.
- 10) N. M. O'Boyle, A. L. Tenderholt, K. M. Langner, *J. Comp. Chem.*, 2008, 29, 839.